

# Uniaxial magnetocrystalline anisotropy in $\text{CaRuO}_3$

Moty Schultz and Lior Klein

*Department of Physics, Bar Ilan University, Ramat Gan 52900, Israel*

J. W. Reiner\* and M. R. Beasley

*Department of Applied Physics, Stanford University, Stanford*

(Dated: November 20, 2018)

$\text{CaRuO}_3$  is a paramagnetic metal and since its low temperature resistivity is described by  $\rho = \rho_0 + AT^\gamma$  with  $\gamma \sim 1.5$ , it is also considered a non-Fermi liquid (NFL) metal. We have performed extensive magnetoresistance and Hall effect measurements of untwinned epitaxial films of  $\text{CaRuO}_3$ . These measurements reveal that  $\text{CaRuO}_3$  exhibits uniaxial magnetocrystalline anisotropy. In addition, the low-temperature NFL behavior is most effectively suppressed when a magnetic field is applied along the easy axis, suggesting that critical spin fluctuations, possibly due to proximity of a quantum critical phase transition, are related to the NFL behavior.

PACS numbers: 72.15.Gd; 71.27.+a; 73.61.-r; 73.50.-h

## I. INTRODUCTION

$\text{CaRuO}_3$  is a paramagnetic metal that attracts considerable attention due to its intriguing properties; in particular, its low temperature resistivity described by  $\rho = \rho_0 + AT^\gamma$  with  $\gamma \sim 1.5$  [1] and its non-Drude optical conductivity [2]. These properties suggest that  $\text{CaRuO}_3$  is a non-Fermi liquid (NFL) metal and since proximity to a magnetic quantum critical point could be the source of this behavior, it is important to elucidate the magnetic properties of  $\text{CaRuO}_3$ .

Here we present measurements of untwinned  $\text{CaRuO}_3$  films and clearly demonstrate for the first time that  $\text{CaRuO}_3$  exhibits anisotropic paramagnetic susceptibility that could be described in terms of an anisotropic susceptibility tensor with the easy axis of magnetization at 45 degrees out of the film plane. This kind of anisotropy is also exhibited by a related compound, the itinerant ferromagnet  $\text{SrRuO}_3$ , in its paramagnetic phase [3].

Direct magnetic measurements of magnetic properties of paramagnetic films suffer from signal weakness combined with large background signal of the substrates. Therefore, we use indirect magnetic measurements where the magnetic properties are inferred from measurements of magnetoresistance (MR) and extraordinary Hall effect (EHE).

Following the identification of the magnetic properties of  $\text{CaRuO}_3$  films, we found that suppression of the low-temperature non-Fermi liquid behavior by external magnetic field is most efficient when the field is applied along the easy axis of magnetization; suggesting that spin fluctuations are related to the NFL behavior.

Our samples are patterned thin films grown either on  $\text{SrTiO}_3$  or on  $\text{NaGaO}_3$ . The measurements presented here are of a 100 nm - thick film of  $\text{CaRuO}_3$  grown on

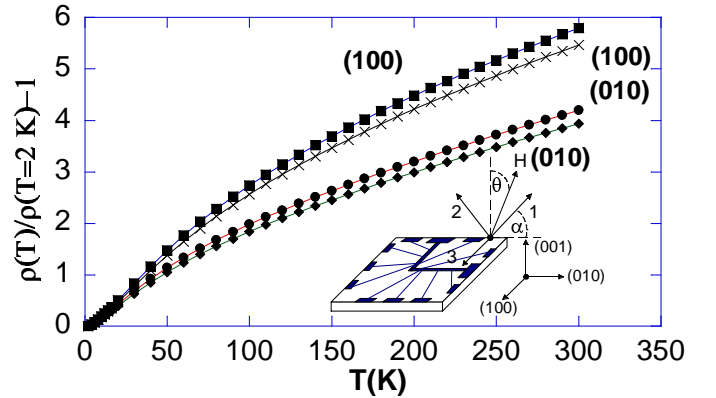


FIG. 1: Rescaled resistivity of four patterns as a function of temperature. In two patterns the current is along [100] while in the other two the current is along (010). Inset: A sketch of the patterned film. The crystallographic directions 1 (easy axis), and 2 (hard axis) are at  $45^\circ$  out of the plane of the film.

slightly miscut ( $\sim 0.3^\circ$ )  $\text{NaGaO}_3$  substrate with resistivity ratio of  $\sim 6.5$ . Resistivity measurements of four different patterns on the same film reveal correlation between resistivity curves and current direction (Figure 1). This indicates that in the films grown on miscut substrates the intrinsic anisotropy is not averaged by twinning. Similar methods, enabled growing of untwinned  $\text{SrRuO}_3$  films. For convenience, we note in the following the miscut direction as the (010) direction of the substrate.

## II. MEASUREMENTS

The magnetic anisotropy of  $\text{CaRuO}_3$  is manifested in MR measurement shown in Figures 2 and 3. The MR is measured as a function of  $\theta$  (See Figure 1) which is the angle between the applied field and the normal to the film with the axis of rotation (100) (Figure 2) or (010) (Figure

\*Present address: Department of Applied Physics, Yale University, New Haven, Connecticut 06520-8284

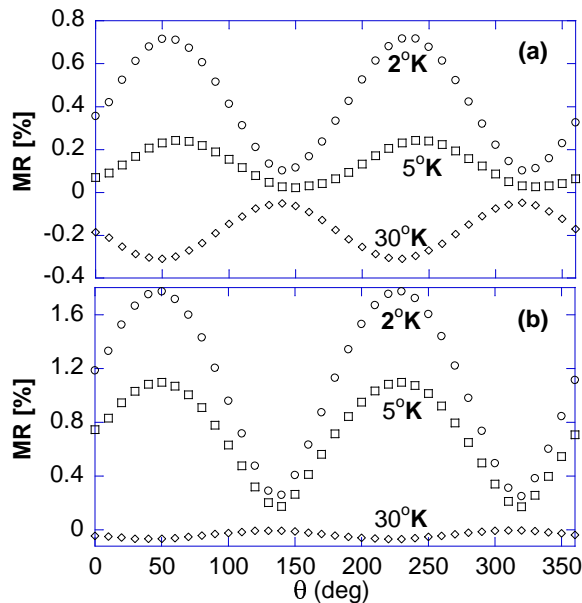


FIG. 2: MR data at 2 K, 5 K and 30 K for  $\mathbf{H}=3$  T as a function of the angle  $\theta$  between  $\mathbf{H}$  and the normal to the sample in the (100) plane. (a) Pattern with current path along the (010) direction. (b) Pattern with current path along the (100) direction.

3). We note that at low temperatures the MR is positive while at high temperatures the MR is negative. Although the temperature at which the MR changes its sign and the values of the MR depend on the current direction and the magnetic field direction, the patterns with current paths along different directions exhibit nonetheless the same qualitative angular dependence: with rotation axis along (100) the graph extrema are at  $\theta = \frac{\pi}{4} + \frac{n\pi}{2}$  while with rotation axis along (010) the graph extrema are at  $\theta = \frac{n\pi}{2}$ . This indicates that the dominant source of MR is related to the orientation of the applied field relative to the epitaxial film irrespective of current direction.

The observed MR cannot be attributed to Lorentz MR. At high temperatures the MR is negative while Lorentz MR is positive. At low temperatures, the MR is positive; however, it is strongly temperature dependent, which is not expected for Lorentz MR where the resistivity hardly changes. For example between 5 K to 2 K the resistivity changes by less than 5% while the MR changes by more than 100%. Moreover, the estimated mean free path even in the zero temperature limit ( $\sim 30\text{\AA}$ ) [4] is much smaller than the cyclotron radius ( $\sim 1\mu\text{m}$ ).

Since Lorentz MR is excluded, we look for MR effects related to the magnetization. Although anisotropic MR is important in this material, it cannot be the dominant effect, since the qualitative angular dependence of the MR is insensitive to the current direction relative to the field. Therefore, a likely source is MR which is sensitive to the magnitude of the magnetization.

At temperatures above  $\sim 10$  K the MR is negative

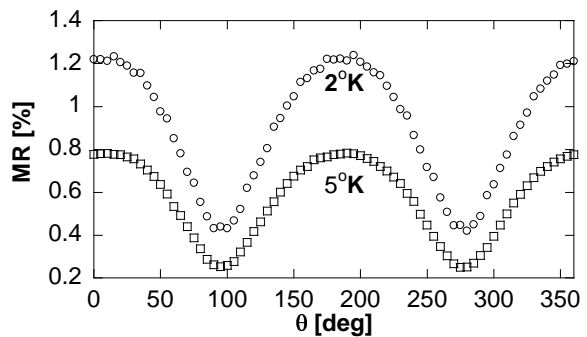


FIG. 3: MR data for current path along the (100) direction at 2 K and 5 K for  $\mathbf{H}=3$  T as a function of the angle  $\theta$  between  $\mathbf{H}$  and the normal to the sample in the (010) plane.

and it can be attributed to suppression of spin fluctuations. Hence, the angular dependence of the MR reflects anisotropic susceptibility of  $\text{CaRuO}_3$  with the easy axis at (011) and the two other principal axes at  $(0\bar{1}1)$  and (100). This explains the observation that for rotation around (100) the graph extrema are at  $\theta = \frac{\pi}{4} + \frac{n\pi}{2}$  while rotation around (010) yields graph extrema at  $\frac{n\pi}{2}$ .

At low temperatures the MR is positive (yet not related to Lorentz MR) and the angle of maximum negative MR at  $T > 10$  K turns into the angle of maximum positive MR at  $T < 10$  K. Since the source of the positive MR is unclear at this stage we need other measurements to determine if the maximum of positive MR also coincides with maximum magnetization. Namely, to determine whether the easy axis at  $T > 10$  K is also the easy axis at  $T < 10$  K. We thus turn to measurements of extraordinary Hall effect.

The Hall field in magnetic conductors, ferromagnetic and paramagnetic, has two contributions:

$$\mathbf{E}_H = -R_0\mathbf{J} \times \mathbf{B} - R_S\mu_0\mathbf{J} \times \mathbf{M} \quad (1)$$

where  $\mathbf{B}$  is the magnetic field, and  $R_0$  and  $R_S$  are the ordinary and the extraordinary Hall coefficient, respectively. The angular dependence of the ordinary Hall effect (OHE) is simple and follows the perpendicular component of  $\mathbf{B}$ . On the other hand, the EHE depends on the perpendicular component of  $\mathbf{M}$  whose magnitude depends (in the presence of uniaxial anisotropy) on the angle between the field and the easy axis. Figures 4a and 4b present the total Hall effect (HE) as a function of  $\theta$  for (100) plane and (010) plane, respectively, for several temperatures. The ordinary Hall Effect is proportional to  $\cos\theta$  while the measured HE has  $\cos(\theta + \varphi)$  dependence (Figure 4a); hence, OHE alone cannot explain the observed angular dependence. Similarly, EHE cannot account for the results without the magnetocrystalline anisotropy.

Quantitatively, the magnetic anisotropy is expressed by an anisotropic susceptibility tensor,  $\tilde{\chi}$  with the mag-

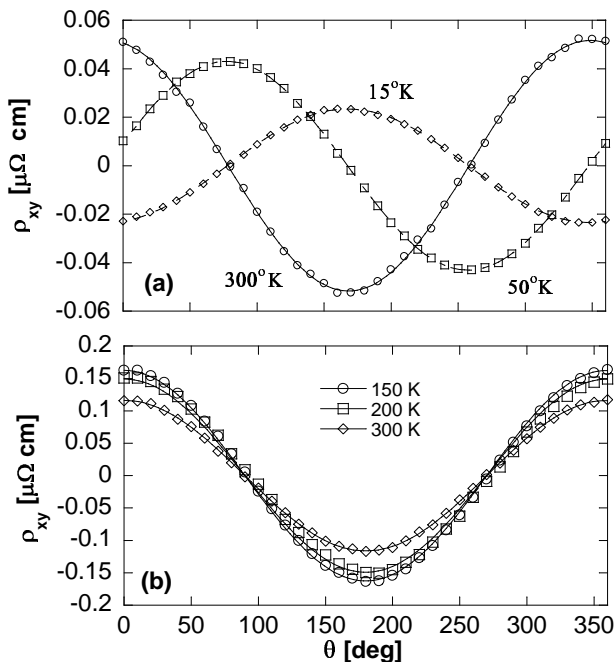


FIG. 4: HE data as a function of the angle  $\theta$  between  $\mathbf{H}$  and the normal to the sample in the (100) plane at  $\mathbf{H} = 4$  T with curves that are fit of  $\cos(\theta + \varphi)$  (a) and in the (010) plane at  $\mathbf{H} = 8$  T with curves that are fit of  $\cos \theta$  (b).

netization vector given by

$$\mu_0 \mathbf{M} = \tilde{\chi} \mathbf{H} \quad (2)$$

where  $\tilde{\chi}$  is the susceptibility tensor with eigenvalues  $\chi_1, \chi_2, \chi_3$ , corresponding to a field applied along the three principal axes. Because (100) is in the plane of the film, our HE measurements are not sensitive to  $\chi_3$ . However, MR measurements indicate that  $\chi_2 \sim \chi_3$ .

With this notation the dependence of the total HE on the angle of the applied field  $\theta$  in the (100) plane ( $\theta$  measured from the normal to the plane of the film) is expected to be:

$$\begin{aligned} \rho_{xy} &= \cos \theta H [R_0 + R_S (\chi_1 \sin^2 \alpha + \chi_2 \cos^2 \alpha)] + \\ &\quad \sin \theta H R_S [\chi_1 - \chi_2] \sin \alpha \cos \alpha = \\ &= \frac{1}{2} H (R_1 + R_2) \cos \theta + \frac{1}{2} H (R_1 - R_2) \sin \theta \end{aligned} \quad (3)$$

and in the (010) plane is:

$$\begin{aligned} \rho_{xy} &= \cos \theta H [R_0 + R_S (\chi_1 \sin^2 \alpha + \chi_2 \cos^2 \alpha)] = \\ &= \frac{1}{2} H (R_1 + R_2) \cos \theta \end{aligned} \quad (4)$$

where  $R_1 = R_0 + R_S \chi_1$ ,  $R_2 = R_0 + R_S \chi_2$  and  $\alpha = 45^\circ$  (See Figure 1). The curves in Figures 4a and 4b are fits to Equations 3 and 4, respectively. As we can see, the fits are satisfactory: At all temperatures the HE in the (100) plane behaves as  $\cos(\theta + \varphi)$  while in the (010) plane as  $\cos \theta$ .

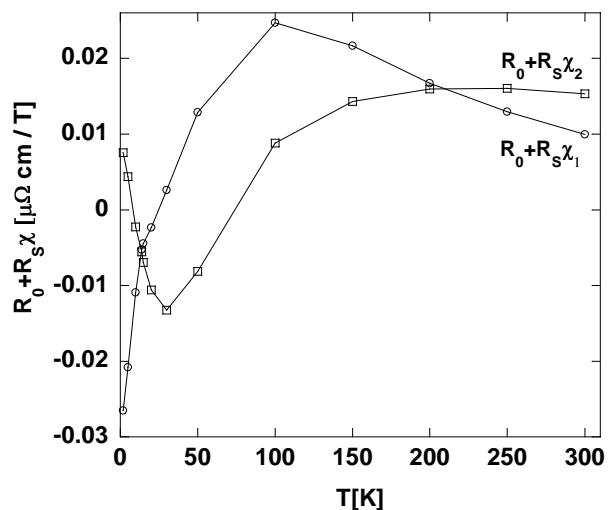


FIG. 5:  $R_0 + R_S \chi_1$  and  $R_0 + R_S \chi_2$  as a function of temperature

As seen in Figure 5,  $R_1$  and  $R_2$  are equal at  $\sim 14$  K and  $\sim 200$  K. There are two possible causes for the identical values: either the EHE vanishes, ( $R_S = 0$ ), or the anisotropy vanishes, ( $\chi_1 = \chi_2$ ). The angular-dependent MR at  $\sim 14$  K indicates that  $\chi_1 \neq \chi_2$ ; hence  $R_S$  changes its sign at  $\sim 14$  K. The MR at  $\sim 200$  K is too small to measure; therefore, we cannot refute either possibility. Nevertheless, the fact that magnetic anisotropy is observed at higher temperatures suggests vanishing of  $R_S$  at 200 K.

If the two crossing points of  $R_0 + R_S \chi_1$  and  $R_0 + R_S \chi_2$  are both due to sign change of  $R_S$ , it means that in the entire temperature interval that we measure  $\chi_1 > \chi_2$ . This means that in CaRuO<sub>3</sub> the easy axis is the (011) direction which is in our film at angle  $\alpha \sim 45^\circ$  relative to the plane of the film, as illustrated in Figure 1. The two other axes are along (0 $\bar{1}$ 1) and (100) directions. This means that the maximum positive MR is correlated with maximum of magnetization. We discuss below possible source of such behavior.

The temperatures at which  $R_S$  vanishes enable convenient measurements of  $R_0$ . Using the most naive one-band calculations  $R_0 = (nqc)^{-1}$ , where  $q$  is the carrier charge and  $n$  is the carrier density, the estimated carrier density is  $n \approx 1.2 \times 10^{23} \text{cm}^{-3}$  of electrons at  $\sim 14^\circ \text{K}$ , and  $n \approx 3.8 \times 10^{22} \text{cm}^{-3}$  of holes at  $\sim 200^\circ \text{K}$ . Since the Hall coefficient shows both signs, both electronlike and holelike bands contribute to the conductivity.

Since proximity to a magnetic quantum critical point could be the source of the NFL behavior in CaRuO<sub>3</sub>, we explore the field dependence of  $\gamma$ . Figure 6 shows  $\gamma$  as a function of field when the field is applied along various directions. The largest increase of  $\gamma$  is obtained for magnetic fields applied along the easy axis, while the smallest increase is obtained for magnetic fields applied along the hard axes. These results indicate that increasing the magnetization is a route of turning CaRuO<sub>3</sub> into

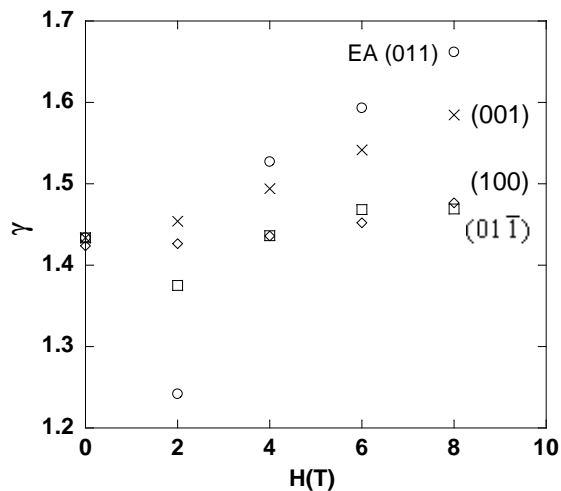


FIG. 6:  $\gamma$  as a function of the magnetic field,  $\mathbf{H}$ , applied along three different orientations.

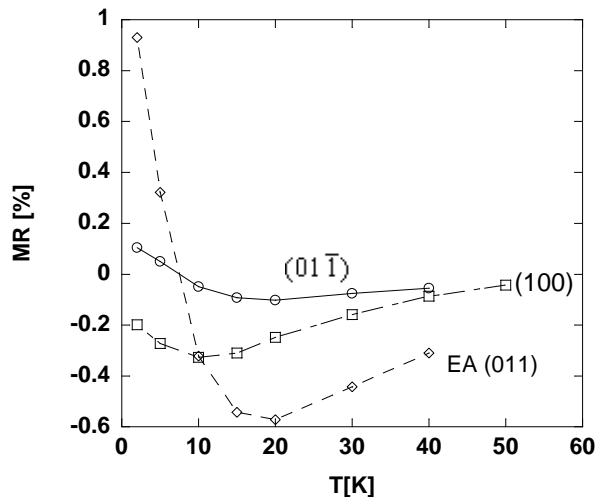


FIG. 7: MR data as a function of temperature at  $\mathbf{H} = 4T$ .

a Fermi liquid metal.

Figure 7 presents the MR with the field applied along the three principal axes as a function of temperature. As shown in Figure 2 at low temperatures the maximum of the positive MR is when the field is applied along the easy axis,  $\theta \approx 45^\circ$ , and at high temperatures the maximum of the negative MR is also obtained when the field is applied along the easy axis. These results imply that the negative

MR, as well as the positive MR, are related to  $\mathbf{M}$  and not to  $\mathbf{H}$ . It is important to note that the temperature at which the MR changes its sign depends on the field and current directions.

### III. DISCUSSION

As mentioned above, the MR is positive at low temperatures and negative at high temperatures, and both, the negative and the positive MR are related to the magnetization and not to the magnetic field. In addition, at all temperature range  $\chi_1 > \chi_2$ . Therefore, the cause for the sign change has to be due to two mechanisms both relating the magnetization to the MR effect.

The negative MR is commonly found in magnetic metals, the applied field suppresses the spin fluctuations, thus yielding negative MR.  $\text{CaRuO}_3$  is a paramagnetic metal. Therefore, one may expect spin contribution to resistivity and hence negative MR.

On the other hand, magnetization related positive MR is less understood. We propose that a possible source for this behavior is the correlation between magnetization and band structure. Electronic structure calculations of  $\text{CaRuO}_3$  using the linear muffin-tin orbital method show a sharp peak in the density of states (DOS) near Fermi level [4]. Therefore, a possible source for the positive MR could be the large variations of the DOS at the Fermi energy. The conductance in metals is proportional to the density of states at the Fermi level, therefore applying a magnetic field on  $\text{CaRuO}_3$  which at low temperature is on the edge of spontaneous splitting of the spin up and spin down bands can change the conductance of the metal. If the maximum of the DOS is at the fermi energy at zero magnetic field then applying magnetic field may reduce the DOS and hence cause positive MR.

The field-induced change in the DOS could be another factor (in addition to suppressing of critical spin fluctuations expected near quantum phase transition) in the partial recovery of Fermi liquid (FL) behavior in  $\text{CaRuO}_3$ . In some NFL metals, like  $\text{CeCu}_{5.9}\text{Au}_{0.1}$  [5],  $\text{CeCuSi}_2$  and  $\text{CeNi}_2\text{Ge}_2$  [6] the FL behavior is recovered at large magnetic fields. Here at  $\mathbf{H} = 8$  T although the FL behavior is not recovered,  $\gamma$  is getting closer to the FL value of 2.

### IV. ACKNOWLEDGMENTS

L.K. acknowledges support by the Israel Science Foundation founded by the Israel Academy of Science and Humanities.

- 
- [1] L. Klein, L. Antognazza, T. H. Geballe, M. R. Beasley, and A. Kapitulnik, Phys. Rev. B **60**, 1448 (1999).  
 [2] Y. S. Lee, J. Yu, J. S. Lee, T. W. Noh, T. H. Gimm, H. Y. Choi and C. B. Eom, Phys. Rev. B **66**, 41104 (2002).  
 [3] Y. Kats, I. Genish, L. Klein, J. Reiner, M. R. Beasley,

- cond-mat/0311341 (2003).  
 [4] G. Santi and T. Jarlborg, J. Phys.: Cond. Matter. **9**, 9563 (1997).  
 [5] H. von Lohneysen, T. Pietrus, G. Portisch, H. G. Schlager, A. Schroder, M. Sieck and T. Trappmann, Phys. Rev. Lett.

- 72**, 3262 (1994).
- [6] F. Steglich, B. Buschinger, P. Gegenwart, M. Lohmann, R. Helfrich, C. Langhammer, P. Hellmann, L. Donnevert, S. Thomas, A. Link, C. Geibel, M. Lang, G. sparn and W. Assmus, *J. Phys.: Cond. Matter.* **8**, 9909 (1996).